

## 1 Introduction and Scientific Motivation

The majority of luminous QSOs expel gas in high velocity ( $0.1\text{--}0.3c$ ) winds as well as accreting it through a disk. In roughly 10–15% of optically selected QSOs we view these winds directly along our line of sight; these objects have rest-frame ultraviolet (UV) spectra showing deep, wide absorption lines that are displaced to the blue of their corresponding emission lines. Such Broad Absorption Lines (BALs) usually correspond to the high-ionization transitions of C IV, Si IV, N V, and O VI, but sometimes the lower-ionization transitions of Mg II and Al III are also seen. The most frequently discussed geometry has the BAL material arranged in an equatorial fan as an outflow radiatively driven off the accretion disk or torus. While it has been difficult to pin down the details of the outflow geometry, the BAL region is clearly a **major component of the nuclear environment**. BAL winds have a covering factor of at least 10%, and spectropolarimetric evidence and theoretical arguments suggest that optical samples may be strongly biased against the discovery of BAL QSOs (e.g., Goodrich 1997; Krolik & Voit 1998). If this is the case, the true space density of BAL QSOs is substantially higher than previously thought, and the covering factor of the BAL material would then be 30% or larger. X-ray observations of BAL QSOs have the potential to constrain the column density, ionization state, covering factor, and outflow velocity of the BAL wind (and any associated material). However, as we describe below, the BAL QSO X-ray data available at present are severely limited and inhomogeneous.

**BAL QSO X-ray studies to date:** BAL QSOs are notoriously faint sources in the soft X-ray band (0.1–2.0 keV; e.g., Green et al. 1995; Green & Mathur 1996), and only  $\approx 11$  BAL QSOs have even been detected in X-rays. The observed soft X-ray faintness is believed to be caused by absorption; this may arise in either the BAL wind itself or in postulated ‘hitchhiking gas’ that screens the BAL material from X-ray radiation (e.g., Murray et al. 1995; Proga et al. 2000; see Figure 1a). We have recently observed a sample of 12 BAL QSOs with *ASCA* and *BeppoSAX* to gain access to more penetrating 2–10 keV X-rays (Gallagher et al. 1999; Brandt et al. 1999; Gallagher et al. 2000). By comparison with QSOs of similar optical fluxes, we found the column densities needed to suppress the expected X-ray fluxes of these BAL QSOs are often very large with  $N_{\text{H}} > 5 \times 10^{23} \text{ cm}^{-2}$ . Furthermore, there is good evidence that the X-ray absorber in at least one BAL QSO, PG 0946+301, is ‘Compton thick’ with  $N_{\text{H}} \gtrsim 10^{24} \text{ cm}^{-2}$  (Mathur et al. 2000). However, in a recent *ASCA* observation, we directly measured the column density for the BAL QSO PG 2112+059 and found it to be  $\approx 50\text{--}100$  times smaller,  $N_{\text{H}} \approx 10^{22} \text{ cm}^{-2}$  (Gallagher et al. 2000). Different absorption column densities are likely to arise from different lines of sight through the outflowing BAL wind (and ‘hitchhiking gas’) as well as intrinsically different outflows.

**What influences observed BAL QSO X-ray emission?** The column density of BAL material and ‘hitchhiking gas’ along the line of sight is certainly a significant factor in determining observed X-ray flux. However, several other BAL QSO properties are almost certainly important as well. In particular, the ionization level of the outflow, the amount of electron scattering in the nucleus, and the inherent strength and spectral shape of the underlying X-ray emission are all expected to affect observed X-ray brightness. Spectral properties in the UV and optical such as absorption line characteristics should reflect these inherent differences, but currently there is no way of reliably predicting which BAL QSOs will be X-ray bright.

The X-ray properties of BAL QSOs as a whole are poorly constrained, and the interesting objects studied to date may not provide a complete picture. A large, systematic sample of sensitive BAL QSO observations above 2 keV would be a significant and efficient contribution to our understanding of the X-ray emission from BAL QSOs.

## 2 Proposed Observations: A BAL QSO Survey for All

We propose to greatly enlarge the number of BAL QSOs with known basic X-ray properties with 35 ACIS-S observations of a well-defined sample. These data will go **public immediately** so that the scientific community will have access to this unprecedented sample of sensitive, high-quality X-ray BAL QSO observations. We will exploit the sensitivity of ACIS to detect high-energy X-rays that penetrate through the X-ray absorbing material. We have selected all the secure BAL QSOs from the Large, Bright Quasar Survey (LBQS; Foltz et al. 1989; Hewett et al. 1995) with  $z > 1.35$  which are not accepted *Chandra* or *XMM-Newton* targets; only two such objects are already targets. The lower limit on redshift was chosen so that the definitive C IV BAL is shifted into the wavelength

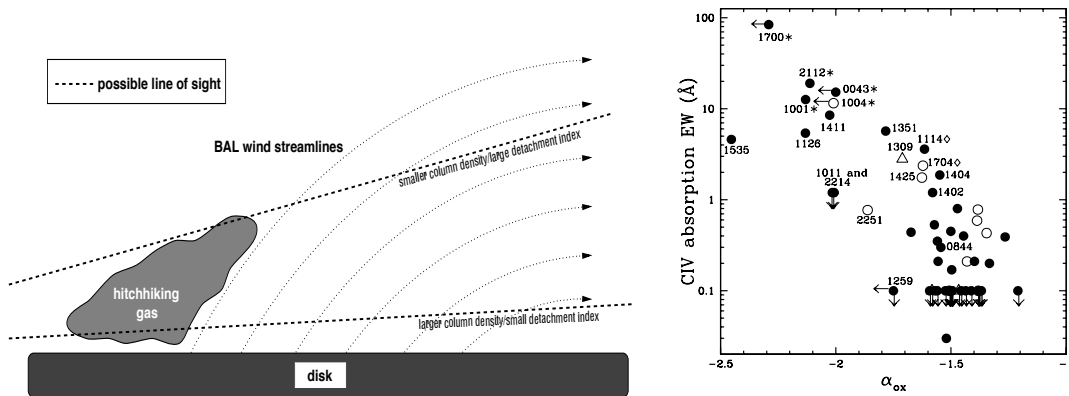


Figure 1: **(a)** Schematic illustration of an accretion disk wind model for BAL QSOs. Matter from the disk is accelerated by radiation pressure. The black hole and X-ray source (not shown) are to the left, and solid curves indicate BAL wind streamlines. The stalled, ‘hitchhiking gas’ absorbs soft X-rays and shields the BAL flow. Adapted from Murray et al. (1995). **(b)** C IV absorption EW versus  $\alpha_{\text{ox}}$  for the Palomar-Green QSOs with  $z < 0.5$ . The BAL QSOs are starred. From Brandt, Laor, & Wills (2000).

range accessible to ground-based spectroscopy; thus our sample contains *all* the BAL QSOs in the LBQS with  $z > 1.35$ . Our targets are optically bright with  $B$  magnitudes from 16.7–18.9, and they are drawn from a homogeneous, magnitude-limited sample that has effective, well-defined and objectively applied selection criteria (see Hewett et al. 1995). Our targets’ redshifts range from 1.41–2.88, and several low-ionization BAL QSOs are included.

We propose exploratory 5–7 ks ACIS observations of each target; our goal is to systematically survey a well-defined sample of BAL QSOs rather than just study a few of them. The excellent spatial resolution of ACIS effectively eliminates background contamination which permits sensitive observations to be carried out in a relatively short time. As we show below, in 5 ks ACIS will probe down to a 2–10 keV flux level of  $\approx 4 \times 10^{-14}$  erg cm $^{-2}$  s $^{-1}$ , and we expect that this sensitivity level will be needed to obtain detections for a large fraction of our targets.

**Science goals:** Our observations will provide the best constraints to date on the intrinsic X-ray absorption/emission of BAL QSOs as a class. For each target, we will have access to highly penetrating X-rays with energies  $\gtrsim 20$  keV and therefore sensitivity to the underlying hard continuum. Even with just a few photons and reasonable assumptions about the underlying X-ray spectrum,  $\alpha_{\text{ox}}$  can be measured and used as a tracer of X-ray absorption (e.g., Brandt, Laor, & Wills 2000; Gallagher et al. 2000).<sup>1</sup> The range of  $\alpha_{\text{ox}}$  seen in normal QSOs is  $-1.7 < \alpha_{\text{ox}} < -1.3$ , but BAL QSOs typically have  $\alpha_{\text{ox}} < -2.0$  (e.g., Green & Mathur 1996; Brandt, Laor, & Wills 2000; see Figure 1b).

Systematic ACIS observations of such a well-defined BAL QSO sample will let us draw general conclusions that are applicable to the BAL QSO population as a whole. Several specific predictions with fundamental implications for the physics of the BAL wind have been proposed; these relate X-ray absorption (and thus  $\alpha_{\text{ox}}$ ) with observables in other wavelength regimes. With our proposed observations, we can directly probe each of them.

**1. Large BAL detachment index will be related to  $\alpha_{\text{ox}}$ .** Detachment index was defined by Weymann et al. (1991; hereafter W91) to indicate the velocity separation of the C IV absorption trough from its corresponding emission line and is a measure of the minimum line-of-sight velocity of the BAL wind. Murray et al. (1995) have put forward a model in which stalled gas ‘hitchhiking’ at the base of the BAL wind absorbs most of the emitted soft X-rays. This protects the BAL wind from becoming completely ionized, and UV photons can then drive the BAL wind radiatively. In this scenario, the strongest X-ray absorption (most negative values of  $\alpha_{\text{ox}}$ ) would coincide with the smallest detachment indices. Physically, this arises when the line of sight is nearly in the equatorial plane, has a long path-length through the X-ray absorbing gas, and also samples relatively small minimum outflow velocities (see Figure 1a). Our targets in the W91 sample have detachment indices

<sup>1</sup>The parameter  $\alpha_{\text{ox}}$  is the spectral index of a hypothetical power law between 2500 Å and 2 keV, and a large, negative value indicates relatively weak X-ray emission.

| Name <sup>a</sup> | $z$   | $B$  | Gal. $N_{\text{H}}^{\text{b}}$ | Notes <sup>c</sup> | Name        | $z$   | $B$  | Gal. $N_{\text{H}}$ | Notes |
|-------------------|-------|------|--------------------------------|--------------------|-------------|-------|------|---------------------|-------|
| GROUP 1           |       |      |                                |                    |             |       |      |                     |       |
| 0019+0107         | 2.128 | 18.1 | 3.2                            | W,P                | 1231+1320†  | 2.380 | 18.8 | 2.6                 | W,P   |
| 0021-0213†        | 2.294 | 18.7 | 2.9                            | W,P                | 1235+0857*  | 2.880 | 18.0 | 1.7                 | W,P   |
| 0025-0151         | 2.078 | 18.1 | 2.8                            | W,P                | 1239+0955   | 2.020 | 18.2 | 1.6                 | W,P   |
| 0029+0017†        | 2.229 | 18.6 | 2.8                            | W,P                | 1331-0108   | 1.870 | 17.9 | 2.2                 | W,P   |
| 1029-0125         | 2.039 | 18.4 | 4.8                            | W,P                | 1442-0011   | 2.202 | 18.2 | 3.6                 | W,P   |
| 1205+1436*        | 1.638 | 18.5 | 2.6                            | W,P                | 1443+0141*  | 2.448 | 18.2 | 3.3                 | W,P   |
| 1208+1535         | 1.943 | 18.1 | 2.7                            | W,P                | 2154-2005   | 2.035 | 18.1 | 2.7                 | W,P   |
| 1212+1445         | 1.638 | 18.0 | 2.7                            | W,P                | 2350-0045A* | 1.617 | 18.6 | 3.1                 | W,P   |
| GROUP 2           |       |      |                                |                    |             |       |      |                     |       |
| 1216+1103         | 1.616 | 18.4 | 2.1                            | W                  | 1314+0116†  | 2.688 | 18.6 | 2.0                 | W     |
| 1235+1453†        | 2.681 | 18.6 | 2.4                            | W                  | 2201-1834   | 1.810 | 17.8 | 2.8                 | W     |
| 1240+1607†        | 2.358 | 18.9 | 2.1                            | W                  | 2211-1915   | 1.952 | 18.0 | 2.3                 | W     |
| 1243+0121†        | 2.796 | 18.5 | 1.7                            | W                  |             |       |      |                     |       |
| GROUP 3           |       |      |                                |                    |             |       |      |                     |       |
| 0004+0147         | 1.711 | 18.1 | 3.0                            |                    | 1203+1530*  | 1.620 | 18.8 | 2.8                 | P     |
| 0010-0012*        | 2.152 | 18.5 | 3.1                            |                    | 1230+1705   | 1.408 | 18.5 | 2.2                 | P     |
| 0051-0019*        | 1.706 | 18.7 | 3.2                            |                    | 2111-4335   | 1.700 | 16.7 | 3.6                 |       |
| 0054+0200         | 1.863 | 18.4 | 3.1                            |                    | 2116-4439   | 1.470 | 17.7 | 3.7                 |       |
| 0109-0128         | 1.749 | 18.3 | 4.0                            |                    | 2140-4552   | 1.700 | 18.3 | 2.5                 |       |
| 1133+0214         | 1.456 | 18.4 | 2.6                            |                    | 2358+0216*  | 1.856 | 18.6 | 3.3                 |       |

Table 1: BAL QSO targets for LBQS *Chandra* survey. All targets have  $z > 1.35$  and are not scheduled to be observed by *Chandra* or *XMM-Newton*. <sup>a</sup> Requesting 5 ks observations unless otherwise indicated: \*6 ks; †7 ks. <sup>b</sup> In units of  $10^{20} \text{ cm}^{-2}$ . <sup>c</sup> Data available in the literature (see §2). W: Spectroscopy, Weymann et al. (1991); P: Polarimetry, HLR98; Lamy & Hutsemékers (2000).

spanning a factor of more than 20, and this survey would allow a direct test of the ‘hitchhiking gas’ model.

**2. BAL QSOs with high optical continuum polarization are more likely to be X-ray bright.** In this scenario, optical continuum polarization arises from electron scattering in the nucleus. This electron ‘mirror’ might also efficiently scatter X-rays around an almost Thomson-thick absorbing outflow, and then these scattered X-rays can be detected. There is some suggestion that the highly polarized BAL QSOs are more likely to be X-ray bright (Gallagher et al. 1999). This possibility was supported by the detection of CSO 755, a BAL QSO with optical continuum polarization of  $\approx 4\%$  (Brandt et al. 1999). Properly testing this connection will provide insight into the geometry of the BAL region (e.g., Goodrich 1997), and there is some evidence that polarization is also related to detachment index (Hutsemékers et al. 1998; hereafter HLR98). Eighteen of our 35 targets have polarization measurements ( $P = 0.2 - 2.3\%$ ) in the literature (see Table 1).

**3. All BAL QSOs should be faint in soft X-rays.** Brandt, Laor, & Wills (2000) found a strong correlation between C IV absorption equivalent width (EW) and  $\alpha_{\text{ox}}$  (see Figure 1b). The QSOs faintest in soft X-rays had the most extreme C IV absorption. This correlation supports the idea that X-ray and UV absorbing gas occur in tandem, though strictly identifying one with the other is still problematic. Since, by definition, all BAL QSOs have large C IV absorption EW, they are all expected to be soft X-ray faint. We can test if this correlation holds at the extreme absorption regime since our objects in W91 have C IV absorption  $\text{EW} = 9-57 \text{ \AA}$  (Hamann, Korista & Morris 1993).

Currently it is not known which BAL QSOs are the X-ray bright ones; our public observations will **identify the X-ray bright BAL QSOs** so that they can be studied by all in subsequent, spectroscopic observations. This should lead to an explosion of discovery in BAL QSO X-ray research! X-ray spectroscopy can determine the column density, ionization state, covering factor, and outflow velocity of the X-ray absorbing material; these quantities are crucial to determine since they set the wind kinetic luminosity and mass outflow rate. Furthermore, spectroscopic measurements of the underlying X-ray continuum will allow direct testing of the idea that BAL QSOs are normal radio-quiet QSOs which happen to be viewed through the outflowing wind.

**Data currently available:** All of our targets already have publicly available optical spectroscopy corresponding to the rest-frame UV, and many of them also have high-quality measurements of their UV absorption-line properties (W91) and optical polarization (HLR98; Lamy & Hutsemékers 2000). The targets are listed in Table 1, and the data available in the literature are indicated in the ‘Notes’

column. The full sample of 35 objects comprises a well-defined set of BAL QSOs as does all of the sources in W91. We have blocked our targets into three groups with decreasing priority in the event that our entire sample of 35 cannot be allocated time in this round. The first group of 16 includes all objects in W91 that also have polarimetric data in the literature; observations of these 16 objects will allow us to make significant headway with our science goals. The second group of 7 includes the remainder of the objects in W91, and the first 16 + 7 = 23 objects constitute the complete sample of W91 objects. The third group (in addition to the two objects already scheduled for *Chandra* and *XMM-Newton* observations) contains the remaining BAL QSOs in the LBQS with  $z > 1.35$ .

**HET support:** In addition, we will obtain nearly simultaneous (rest-frame UV) spectra using the 8-m Hobby-Eberly Telescope (HET; 30% owned by Penn State) for as many of these BAL QSOs as possible. The queue-scheduled HET can observe down to declinations of  $-10^\circ$ ; these observations would include 29 out of the 35 objects in the total sample. With these data, we can measure the BAL properties as well as the rest-frame 2500 Å flux density (for calculating  $\alpha_{\text{ox}}$ ) to prevent uncertainty due to variability. We will make the raw data from these observations available immediately to the public, and we will also provide the reduced spectra as quickly as possible.

**Additional science:** As a side benefit, our BAL QSO survey will provide fairly deep hard X-ray images over  $\approx 1.2 \text{ deg}^2$  of sky already surveyed by the LBQS. These can be used to compare X-ray quasar selection methods to those employed by the LBQS. For example, we should detect several highly-reddened QSOs that were missed by the LBQS if their space density is as high as suggested by Webster et al. (1995).

### 3 Technical Feasibility

**PHL 5200 comparison:** To assess technical feasibility, we first compare our targets with the famous  $z = 1.98$  BAL QSO PHL 5200. PHL 5200, with  $B = 18.2$ , was clearly detected by *ASCA* with a 2–10 keV flux of  $\approx 2.9 \times 10^{-13} \text{ erg cm}^{-2} \text{ s}^{-1}$  (Mathur, Elvis, & Singh 1995). As our ACIS-S observations will probe 7–10 times deeper than this flux (see below) and our targets are comparably bright in  $B$  to PHL 5200 (see Table 1), we expect solid detections or tight upper limits for all targets.

**Expected sensitivity:** We have used PIMMS, MARX, and XSPEC to calculate our 2–10 keV sensitivity level for a 5 ks ACIS exposure. We consider a representative BAL QSO with  $z = 1.8$  (compare with Table 1), an intrinsic neutral absorption column density of  $5 \times 10^{23} \text{ cm}^{-2}$ , an underlying X-ray continuum with  $\Gamma = 1.9$ , and a Galactic column density of  $3 \times 10^{20} \text{ cm}^{-2}$ . Using ACIS, we can detect this BAL QSO provided its 2–10 keV flux is larger than  $4 \times 10^{-14} \text{ erg cm}^{-2} \text{ s}^{-1}$  (here we conservatively use a 12-photon detection criterion; our analyses thus far suggest we can actually use an 8-photon criterion). Since our targets have  $z = 1.41\text{--}2.88$ , we will have sensitivity to hard X-rays up to 20–35 keV. Provided the column densities intrinsic to these BAL QSOs are  $\lesssim 10^{24} \text{ cm}^{-2}$ , we should be able to detect most of the objects in our sample. If we do not detect one of our targets, we can constrain its value of  $\alpha_{\text{ox}}$  to be less than  $\approx -2.2$  with 95% confidence provided it has  $B < 18.6$  (setting upper limits following Kraft, Burrows, & Nousek 1991). Obtaining a sufficient depth in  $\alpha_{\text{ox}}$  is crucial for achieving our science goals. The level of sensitivity is a function of both redshift and  $B$  magnitude, and we request 6 or 7 ks exposures of fainter objects in order to attain at least  $\alpha_{\text{ox}} < -2.0$  (see Table 1). This limit corresponds to 25 times fainter than typical radio-quiet QSOs in 2 keV flux density. In comparison, Green et al. (1995) measured  $\alpha_{\text{ox}}$  for all of the LBQS BAL QSOs with the *ROSAT* All-Sky Survey, and their most sensitive measurement gave  $\alpha_{\text{ox}} < -1.5$ .

We do not expect photon pile up to be significant.

Brandt W.N., et al., 1999, ApJ, 525, L69

Foltz C.B., et al., 1989, AJ, 98, 1959

Gallagher S. C. et al., 1999, ApJ, 519, 549

Gallagher S. C. et al., 2000, ApJ, submitted

Goodrich R.W., 1997, ApJ, 474, 606

Green P.J., et al., 1995, ApJ, 450, 51

Green P.J., Mathur S., 1996, ApJ, 462, 637

Hamann F., Korista K.T., Morris S.L., 1993, ApJ, 415, 541 (HKM93)

Hewett P.C., et al., 1995, AJ, 109, 1498

Hutsemékers D., Lamy H., Remy M., 1998, A&A, 340, 371 (HLR98)

Korista K.T., et al., 1992, ApJ, 401, 529

Kraft R.P., Burrows D.N., Nousek J.A., 1991, ApJ, 374, 344

Krolik J.H., Voit G.M., 1998, ApJ, 497, L5

Lamy H., Hutsemékers D., 2000, A&AS, 142, 451

Laor A., et al., 1997, ApJ, 477, 93

Mathur S., Elvis M., Singh K.P., 1995, ApJ, 455, L9

Mathur S., et al., 2000, ApJ, 533, L79

Murray N., et al., 1995, ApJ, 451, 498

Proga D., et al., 2000, ApJ, in press (astro-ph/0005315)

Stoeckle J.T., et al., 1992, ApJ, 396, 487

Webster R., et al., 1995, Nature, 375, 469

Weymann R.J., et al., 1991, ApJ, 373, 23 (W91)